

FRACTOGRAPHIC OBSERVATIONS IN ASYMMETRIC
AND SYMMETRIC FULLY PLASTIC CRACK GROWTH

G.A. Kardomateas*

Massachusetts Institute of Technology
Cambridge, MA 02139, U.S.A

(Received November 4, 1985)

(Revised February 24, 1986)

Introduction

Observations of ductile fracture suggest that it results from a multi-step process initiated by the cracking of inclusions or the separation of inclusion-metal interfaces, followed by void growth and coalescence. The coalescence has been observed to occur on a plane of high shear stress, giving elongated dimples, or on a plane normal to the direction of maximum tensile stress, giving equiaxed dimples (1,2). Macroscopically, fracture surface orientations at the shear direction of 45° to the maximum tensile stress at initiation and at 90° to this direction at growth have been observed (3, 4) on Charpy V-notch steel specimens in three-point bending. Furthermore, fracture surfaces have been studied to identify and classify the characteristic surface markings that are produced by the deformation mechanisms (5,6).

For the usual symmetric singly grooved plane strain specimens in tension the slip line field consists of two lines at $\pm 45^\circ$ intersecting the tip of the groove. In the asymmetric case only a single shear zone exists (Fig. 1). Such asymmetric configurations may arise if a weld or a harder heat-affected zone or a shoulder on one side eliminates the other shear band. This case shows less ductility than the symmetric case (7), because the crack is advancing into prestrained material along the shear band rather than the new material encountered by a crack advancing between two symmetrical shear zones.

Tests on singly-grooved, fatigue-precracked symmetric and asymmetric (asymmetry introduced through a shoulder) specimens (7) were performed on six alloys for which X-ray spectography gave the predominant inclusions: 1018 cold finished steel with Si-bearing inclusions, 1018 steel normalized at 1700° , A36 hot rolled steel with MnS inclusions, HY80 steel with Al-bearing inclusions, HY100 steel with MnS inclusions and 5056-H111 aluminum with Fe-bearing inclusions. These alloys can be separated into the lower hardening ones such as the 1018 cold finished, HY80 and HY100 steel and the higher hardening ones such as the A36 hot rolled and 1018 normalized steel. It was found (7) that in the lower hardening alloys, the crack ductility, defined as the minimum axial displacement per unit projected ligament reduction, $du_a/d\ell$, is substantially lower in the asymmetric configuration than in the symmetric one. In the higher hardening alloys the crack ductility is almost the same in both geometries. Notice that thinning of the ligament from the far side in fully plastic flow makes the reduction in ligament rather than crack advance more appropriate for describing load drop. In this work the microscopic features of the fracture surfaces for the two geometries are compared.

Results and Discussion

In general, for a given crack tip opening displacement, the amount of crack extension can be separated into two components: a sliding off component and a fracture component. To quantify the ductility, as observed from the fractographs, an "apparent crack ductility", D_{AC} , observed fractographically, can be defined as the ratio of that part of the projected crack area exposed by pure plastic flow to the total projected area, including that exposed by fracture. For instance, with n parabolic dimple markings per unit area, each having tip radius

* Present address: General Motors Research Laboratories, Engineering Mechanics Department, Warren, Michigan 48090-9055

r , the apparent crack ductility may be found by assuming that the area πr^2 of each parabola opens up before arrival of the crack front, and the balance of the surface is formed by sliding off. Then

$$D_{AC} = 1 - \pi r^2.$$

Due to the difficulty in measuring these quantities, only approximate estimations for D_{AC} can be obtained. Table 1 shows these findings (estimated from the fractographs of the upper and lower flank, surface normal to the beam) for the low hardening 1018 cold finished steel and the high hardening A36 hot rolled steel of the asymmetric and symmetric specimens. These values represent the average of three specimens over several regions with an estimated standard deviation about 11% the mean value in these samples. The results of Table 1 are another manifestation of the fact that lower hardening alloys in the asymmetric configuration are less ductile than in the symmetric one, while higher hardening alloys are almost equally ductile in both geometries (7). The apparent crack ductility which is a measure of the relative amounts of sliding off and fracture on the flanks cannot be compared directly with the crack growth ductility, which is based on the mechanical behavior of the specimen (load-extension curves). The fracture geometry can, however, provide a consistent connection through a macro-mechanical model that describes crack growth as a sequence of sliding off and fracture (7). At present, it suffices to say that considering the idealization of the complex hole-crack tip interaction, the main outcome is the common trend of both the macroscopic and microscopic measures of ductility with respect to strain hardening and geometry (reduced ductility with less hardening and in the asymmetric configuration).

TABLE 1

	Apparent Crack Ductility D_{AC} from fractographs		Crack Growth Ductility du_a/dl from (7).
	Lower Flank $D_{AC,l}$	Upper Flank $D_{AC,u}$	
1018 CF steel Asymmetric	0.52	0.37	0.072
1018 CF steel Symmetric	0.67	0.67	0.233
A36 HR steel Asymmetric	0.68	0.57	0.181
A36 HR steel Symmetric	0.68	0.68	0.192

Fig. 2 shows micrographs of the upper and lower flanks for 5086-H111 aluminum with different degrees of void formation and shearing. Fracture is more the "shear type" in the lower flank, indicating a larger sliding off component in the crack extension. Differences in the shapes of mating dimples were also considered in (8) by precision matching of fracture surfaces and were used to indicate the differences in plastic flow on either side of the crack tip during mixed mode crack growth. Furthermore, this suggests a macro-mechanical model for crack growth by combined void growth and sliding off, where the lower flank slides off along the upper slip plane and the upper flank slides off along the lower slip plane by a smaller amount. Thus the lower flank consists of a larger amount of "sheared" material than the upper. Based on this observation, a macro-mechanical model for crack growth can be developed (7) and provide a physical basis for explaining the development of deformation in the asymmetric, mixed Mode I and II case. For the symmetric pure Mode I case the corresponding mechanism consists of equal amounts of sliding off on two symmetric slip planes, followed by fracture.

To compare the symmetric and asymmetric cases, consider Fig. 3 which shows micrographs of the low-hardening 1018 cold finished asymmetric and symmetric specimens. This alloy shows a substantial reduction in ductility in the asymmetric configuration. In the asymmetric case the fracture is more the "shear type" with voids elongated in the direction of crack growth; in the symmetric case the fracture is more the "normal type" with equiaxed voids. In the high-hardening A36 hot rolled steel, with small differences in the ductility between the asymmetric and symmetric cases, the corresponding micrographs (Fig. 4) are not much different: the fracture in the asymmetric case is almost as much the "normal type" as in the symmetric case. A comparison of Figs. 3 and 4 illustrates the effect of strain hardening on the asymmetric (but not the symmetric) fully plastic specimens.

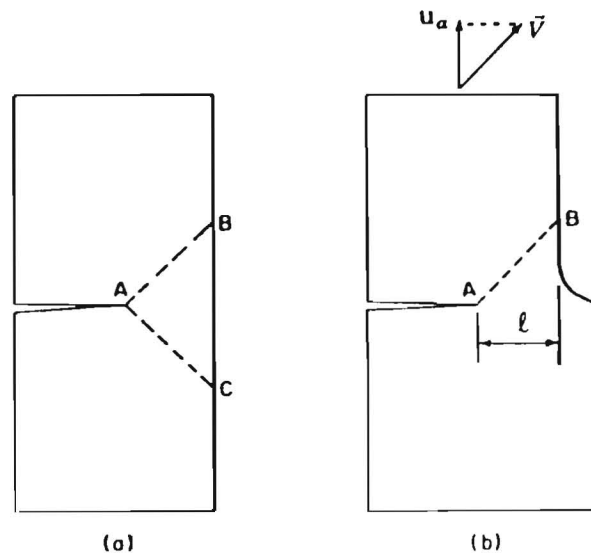


FIG. 1
Symmetric (a) and Asymmetric (b) shear band
configuration from cracks.

A noteworthy feature of some symmetric specimens, where two slip planes are active and the crack grows by alternating shear, is the "zig-zagging" of the fracture surface. In this case a wavy (zig-zag) region follows the fatigue precrack. Microvoid coalescence along alternating shear planes leading to the characteristic zig-zag fracture has also been described in (9) as a continuous blend of Modes I and II.

Conclusions

Fractographic observations of deformation during crack extension in the asymmetric, mixed Mode I and II specimens suggests a mechanism of fracture followed by sliding off along two slip planes; a larger amount of sliding off occurring in the lower flank. The usual symmetric case suggests alternating shear and fracture and in some cases the microscopic surface is characterized by zig-zagging. Noteworthy feature in the low hardening asymmetric specimens is the "shear type" fracture with elongated voids. The corresponding symmetric specimens, with the larger ductility, show in turn the "normal type" fracture with more equiaxed voids. In the higher hardening alloys, which are almost equally ductile for both geometries, the corresponding micrographs are not appreciably different. An "apparent crack ductility", observed fractographically, has also been defined as the ratio of the sliding off area to the total one including fracture.

Acknowledgement

The financial support of the Office of Naval Research, Contract N0014-82K-0025 is gratefully acknowledged.

References

1. J. Gurland and J. Plateau, *Transactions ASM* 56 442 (1963)
2. H.W. Hayden and S. Floreen, *Acta Met.* 17 213 (1969).
3. F. Zia-Ebrahimi, D. K. Matlock and G. Krauss, *Scripta Met.* 16 987 (1982).
4. F. Zia-Ebrahimi and G. Krauss, *Acta Met.* 32 1767 (1984).
5. C.D. Beachem and D.A. Meyn, *ASTM STP* 436 59 (1968).
6. H.C. Rogers, "Fracture", M.I.T. Press (1959).
7. G.A. Kardomateas, Ph.D. thesis, Massachusetts Institute of Technology (1985).
8. C. D. Beachem, *Met. Trans.* 6A 377 (1975).
9. C. D. Beachem and G. R. Yoder, *Met. Trans.* 4A 1145 (1973).

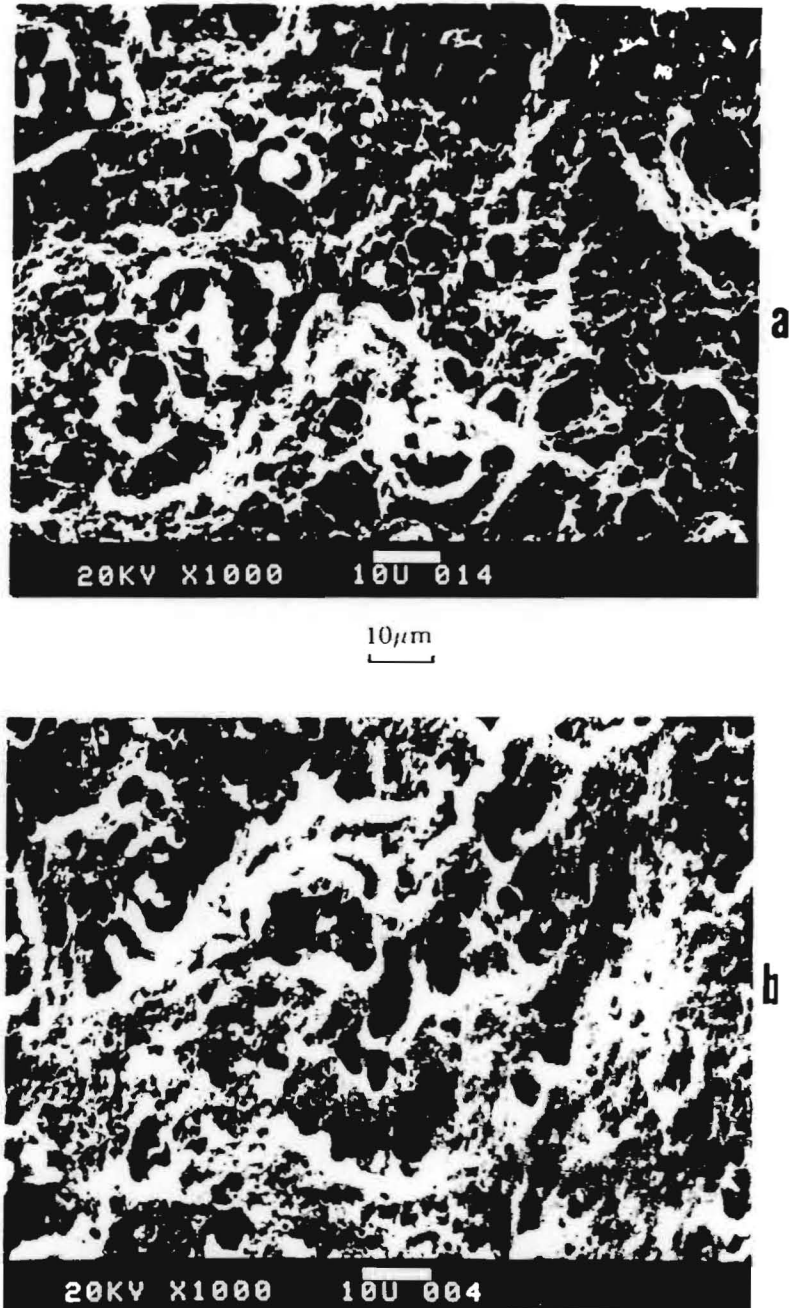


FIG. 2
Fracture surface of 5086-H111 aluminum asymmetric specimen
showing the difference between the two flanks;
(a) Upper flank, (b) Lower flank with more shearing.

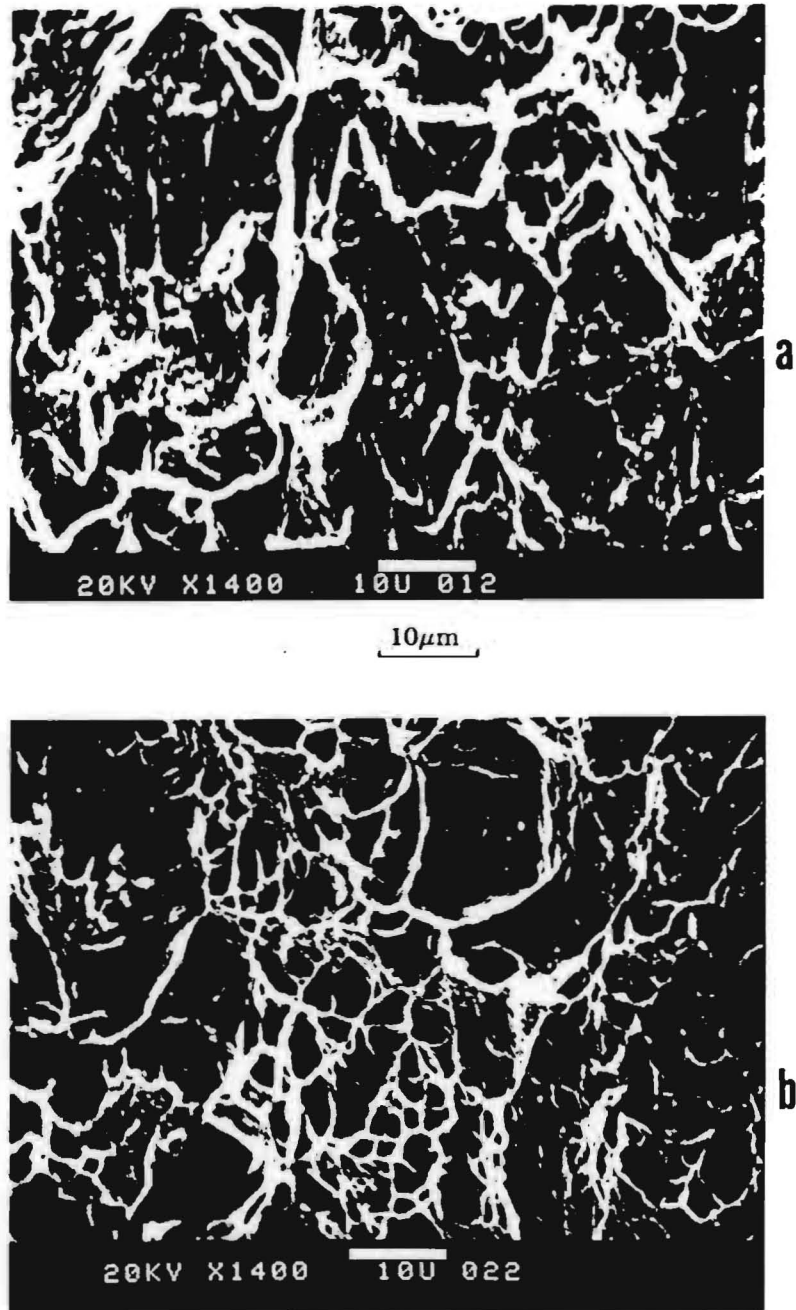


FIG. 3
Fracture surface of 1018 cold finished steel (lower hardening alloy).
(a) Asymmetric, (b) Symmetric: more "shear type" fracture
in the asymmetric, less ductile case.

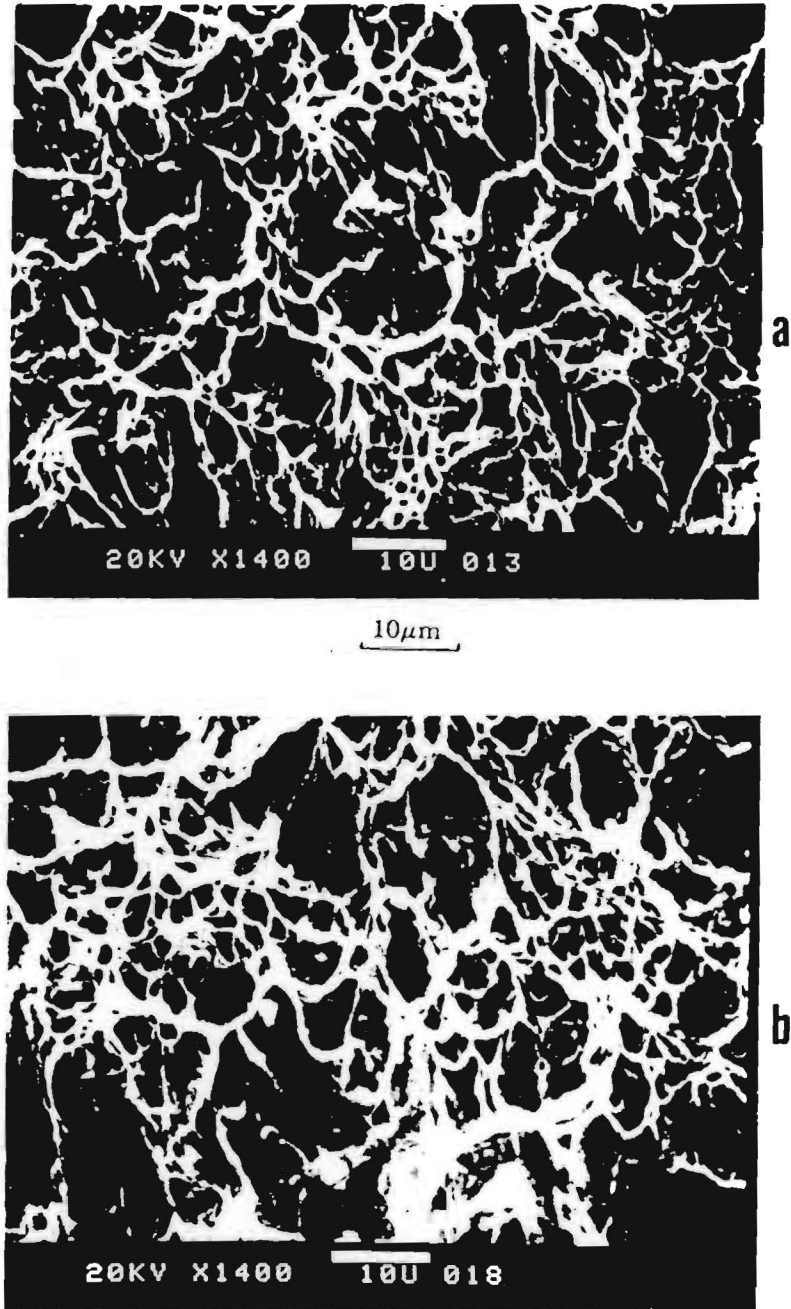


FIG. 4
Fracture surface of A36 hot rolled steel (higher hardening alloy); (a) Asymmetric, (b) Symmetric without appreciable difference. Both cases are almost equally ductile.